12-18-2021

On the thermogravimetric analysis of polymers: Polyethylene oxide powder and nanofibers

Oriretan Omosola

Dorina M. Chipara

Mohammed Jasim Uddin

Karen Lozano

Mataz Alcoutlabi

See next page for additional authors

Authors

Oriretan Omosola, Dorina M. Chipara, Mohammed Jasim Uddin, Karen Lozano, Mataz Alcoutlabi, Victoria Padilla-Gainza, and Mircea Chipara

Chipara Mircea (Orcid ID: 0000-0003-3584-4863)

On the Thermogravimetric Analysis of Polymers: Polyethylene Oxide Powder and Nanofibers

Oriretan Omosola[1], Dorina Magdalena Chipara[2], Mohammad Uddin[1], Karen Lozano[3], Mataz Alcoutlabi[3], Victoria Padilla[3], Mircea Chipara[2*]

[1]Department of Chemistry, College of Sciences, The University of Texas Rio Grande Valley, Edinburg, TX, USA

[2]Department of Physics and Astronomy, College of Sciences, The University of Texas Rio Grande Valley, Edinburg, TX, USA

[3]Department of Mechanical Engineering, College of Engineering and Computer Science, The University of Texas Rio Grande Valley, Edinburg, TX, USA

*Corresponding Author: Mircea Chipara, Department of Physics and Astronomy, College of Sciences, The University of Texas Rio Grande Valley, 1201 W. University Drive, Edinburg, Texas, TX 78539, USA. E-mail address: mircea.chipara@utrgv.edu

ABSTRACT

Thermogravimetric analysis of polyethylene oxide (powder and nanofibers obtained by force spinning water or chloroform solutions of polyethylene oxide) was studied using different theoretical models such as Friedman and Flynn-Wall-Ozawa. A semiempirical approach for estimating the "sigmoid activation energy" from the thermal degradation was suggested and confirmed by the experimental data on PEO powder and nanofibers' mats. The equation allowed for calculating a "sigmoid activation energy" from a single thermogram using a single heating rate without requiring any model for the actual complex set of chemical reactions involved in the thermal degradation process. For PEO (po wder and nanofibers obtained from water solutions), the "sigmoid activation energy" increased as the heating rate was increased. The sigmoid activation energy for PEO mats obtained from chloroform solutions exhibited a small decrease as the heating rate was increased. Thermograms' derivatives were fitted to determine the coordinates of the inflection points. The "sigmoid activation energy" was compared to the activation energy determined from the Flynn-Wall-Ozawa model. Similarities between the thermal degradation of polyethylene oxide powder and of the nanofibers obtained from water

solutions were discussed. Significant differences between the sigmoid activation energies of the mats obtained from water and chloroform solutions were reported.

INTRODUCTION

Many materials and expressly polymers have limited survivability when exposed to high temperatures. The thermogravimetric analysis quantifies the evolution of a polymer mass (weight) as a function of temperature and time when subjected to various temperatures in different environments. The primary environments are 1. The inert atmosphere, achieved by performing the degradation in nitrogen, noble gases, or vacuum. 2. The Earth's atmosphere (which is a combination of nitrogen and oxygen). 3. The reactive atmosphere (which is typically associated with thermal effects in polymers under oxygen or other reactive gases). Thermogravimetric analysis (TGA) is a standard experimental technique used to study thermal phenomena in homopolymers [1], [2], polymer blends [3], copolymers [4], block copolymers [5], polymer-based nanocomposites, and metals [6], [7]. The simplest TGA thermogram (under inert atmosphere) is a single sigmoid representing the dependence of residual mass on temperature. The sigmoid typically has no extremum point. For more complex degradation processes, thermal degradation combines several overlapping sigmoids. In the case of TGA experiments performed in oxygen or reactive gases, the dependence of the residual mass on temperature and time is more complex due to the diffusion contributions, and the new chemical reaction path(s) opened eventually by the reactive gas(es). Recent advanced experimental protocols include the hyphenation of the TGA spectrometer with other instruments such as Fourier Transform Infrared (FTIR) [8] or mass spectrometers [9], [10], which can provide additional information on the nature and composition of volatiles or residues.

The present manuscript focuses on the following three significant aspects of TGA: Firstly, it introduces a quasi-empirical approach for understanding the thermograms by starting from a simple sigmoid and deriving an expression to describe the evolution of residual mass as a function of temperature. This approach assumes that the thermogram is a single sigmoid. Such shape was frequently reported for simple polymers and polymer-based nanocomposites, where the polymeric matrix is a homopolymer and the (nano)filler has high-temperature stability (e.g., carbon nanostructures such as nanotubes, nanofibers, graphite, graphene…).

The choice of PEO powder and mats of nanofibers for this research originated from a few specific features of this polymer. PEO has a simple chemical structure ($C_{2n}H_{4n+2}O_{n+1}$) where n is the number of monomers, a well-known morphology with a semi-crystalline content, well-known glass (-50 ^{o}C [11] or -67 ^{o}C [12]), crystallization (52 ^{o}C [13]), and melting phase transitions (65 ^{o}C [11]), and a simple thermal degradation (in the inert atmosphere [12]), characterized by a low char production. PEO is among the few polymers soluble in water and in some organic solvents such as toluene and chloroform. PEO is considered a biocompatible polymer, thus opening the door towards biological and medical applications.

The proposed equation for the simulation of the residual mass dependence on temperature allows the estimation of an activation energy, named "sigmoid activation energy", without any connection to the actual kinetics of the thermal degradation process. Thus, this approach does not require a detailed analysis of the thermal degradation dependence on the heating rate. Some authors define Ozawa-Flynn-Wall as a "model-free" approach [1], although it includes a function of conversion which may be deemed dependent on the thermo-oxidation path [14], [15]. This contribution affects the intercept but not the slope (identified as the activation energy) of the heating rate logarithm dependence on the reciprocal temperature [1], [14], [15]. Thus the "sigmoid activation energy" may be determined from a single thermogram, recorded at a single heating rate. This is the first theoretical approach capable of finding such a simple path towards activation energy.

Secondly, the results reported in this manuscript demonstrate that the actual thermograms that represent the temperature dependence of the residual mass of a simple homopolymer (PEO) at different heating rates are very well fitted by the proposed equation. The demonstration is extended to PEO nanofibers obtained by force spinning from water or chloroform solutions. Differences between the sigmoid activation energy of the PEO mats of nanofibers, originating from the nature of the solvent are possible (and expected) because the type of solvent may control the morphology of the nanofibers. For example, the activation energy for the crystallization of PEO is greater in the case of samples obtained from dimethyl acetamide (DMAc) and toluene than for tripropionin [16], reflecting different radial nucleation speeds. The effect of solvents on nanofibers of PEO was also reported [17] and confirmed. The degree of crystallinity of PEO nanofibers electrospun from solution decreases as water is gradually replaced by ethanol [17].

In conclusion, a detailed analysis of the similarities and discrepancies between the thermal degradation of polyethylene oxide (PEO) powder and nanofibers is reported.
Finally, the manuscript includes a detailed study of the parameters associated with the derivatives of the as-recorded thermograms (with respect to the temperature). A particular emphasis is given on the inflection temperature, inflection thermal residual mass, and width of the thermal degradation rate.

MATHEMATICAL FRAMEWORK

Thermo-oxidative degradation is a complex phenomenon occurring in both time and temperature. The experimental data represent the residual mass at a given temperature and time during the degradation process. These two main parameters (time and temperature) may be deconvoluted theoretically to simplify the mathematical analysis. In most cases, the thermograms are perceived as dependencies of the thermal residual mass on temperature.
Let "r" be the residual mass of the sample, which depends both on temperature T and time t. Accordingly, define r(t) as the time residual mass, and R(T) as the thermal residual mass

$$r(t) = m(t_0) - m(t) \ \textit{and} \quad R(T) = m(T_0) - m(T) \qquad (1)$$

Where $m(t_0)$ is the mass of the polymer at the beginning of the thermal degradation process, $m(t_\infty)$ is the mass of the polymer at the end of the thermal degradation process, m(t) is the mass of the polymer after a thermal degradation time t, $m(T_0)$ is the mass of the polymer at the beginning of the thermal degradation process, $m(T_\infty)$ is the mass of the polymer at the end of the thermal degradation process, and m(T) is the mass of the polymer at the temperature T.
Standard thermograms depict the dependence of the thermal residual mass on temperature. In the general case, the time residual mass is a function of both time and temperature. However, the subsequent analysis will assume that the time residual mass is just a function of time (unless stated otherwise). This requires the decoupling of the time and temperature contributions, which may be achieved by assuming that the time residual mass r(t) is a function of both time and temperature, represented as t(T). Mathematically, this implies r(t)= r(t(T)). Consequently:

$$\frac{dr}{dt} = \frac{dr\left(t\left(T\right)\right)}{dt} = \frac{\partial r}{\partial T}\frac{\partial T}{\partial t} \approx H\frac{\partial R}{\partial T} \qquad (2)$$

The possibility of such dependence is supported by the presence of the heating rate of the sample $\partial T/\partial t = H$, which couples time and temperature. Equation (2) provides a simple transformation from the time residual mass rate ($\partial r/\partial t$) to the thermal residual mass rate ($\partial R/\partial T$), where R(T) is the thermal residual mass, imagined depending only on temperature (with a negligible time dependence)

Hence, it is natural to imagine that the thermograms are simple sigmoids represented by the following equation (typical for a sigmoid: please see also https://mathworld.wolfram.com/SigmoidFunction.html):

$$R(t) = \frac{A}{1 + B\exp(\alpha t)} \qquad (3)$$

It is observed that for t=0, r(t) function has the value of r(0) =A/(1+B), and at longer times, the asymptotic value will be $r(\infty)\rightarrow 0$, where A, B, and α are assumed to be constants. As expected, this function has no extremum for any finite value of the time, t. In eq. (3), α plays the role of a reaction rate. Hence, such a dependence mimics the dependence of the residual mass on temperature qualitatively. So, it is natural to assume that the reaction rate α has an Arrhenius like temperature dependence:

$$\alpha = \alpha(T) = \alpha_0 exp - \frac{E_A}{K_B T} (4)$$

With:

$$R(t) = \frac{A}{1 + B\exp\left[\left(\alpha_0 exp - \frac{E_A}{K_B T}\right)t\right]} \qquad (4')$$

where E_A is the activation energy, K_B Boltzmann's constant, and T the absolute temperature. At relatively high temperatures T, the exponential may be developed in power series around the origin ($\exp -x \approx 1 - x + x^2/2$). Retaining only the terms up to the first-order is obtained:

$$r(t) = \frac{A}{1 + B\exp\left[\alpha_0\left(1 - \frac{E_A}{K_B T}\right)t\right]} \qquad (5)$$

The next step is to find a relationship between r(t) and R(T). To fulfill this goal, let us consider the expression of the time residual mass r:

$$r(t)=\int_{t_0}^{t}\frac{dr}{dt}dt=\int_{t_0}^{t}\frac{dr}{dT}\frac{dT}{dt}dt \qquad (6)$$

Recognizing that dT/dt is the heating rate H, and assuming a constant heating rate is obtained:

$$\int_{t_0}^{t}\left[\frac{dr}{dt}-H\frac{dr}{dT}\right]dt\approx\int_{t_0}^{t}\left[\frac{dr}{dt}-H\frac{dR}{dT}\right]dt=0 \quad (6')$$

Although equation (2) may be considered as indicating that r(t)≈HR(T), eq. 6' proves that this is a rough approximation. Consequently, by accepting such a crude approximation:

$$R(T)=\frac{r(t)}{H}=\frac{A}{\left\{1+B\left(exp\alpha_0 t\right)\exp\left[-\left(\frac{E_A}{K_B T}\right)\alpha_0 t\right]\right\}H} \quad (6'')$$

The main goal of these transformations is to collect in R(T) the dependence of the thermal residual mass on T so that there will be almost no dependence of R on time. Thus, mathematically, R should be solely a function of temperature T while t should have been converted into a constant parameter. By observing that α_0 is also a small constant, it is assumed reasonably to replace $\alpha_0 t$ by an overall (almost) constant parameter δ as follows:

$$R(T)=\frac{A}{H}\frac{1}{1+B\left(exp\delta\right)\exp\left[-\left(\frac{E_A}{K_B T}\right)\delta\right]} \quad (6''')$$

Assuming that α_0 is very small than $\exp\alpha_0 t \approx 1+\alpha_0 t \approx 1$. This condition will be gently relaxed, and it will be assumed that $\exp\alpha_0 t \approx \delta$, where δ will be considered as a constant. The recorded thermogram is a mathematical graph representing the dependence of the thermal residual mass R on temperature, R=(T).

Eq. (6''') may be simplified by using the notations AH=C and B exp(δ)=D, and absorbing δ into the sigmoid activation energy ($E_A^{(S)} = \delta E_A$):

$$R(T)=\frac{A}{H}\frac{1}{1+Dexp\left[-\left(\frac{E_A^{(S)}}{K_B T}\right)\right]} \quad (7)$$

The parameter δ describes the time-temperature coupling.

To conclude, the thermograms are expected to be well described by equation (7). The best fit of experimental data using equation (7) provides the sigmoid activation energy and not the actual

activation energy for the thermal degradation process. It is possible to estimate the time-temperature coupling parameter, δ, by calculating the activation energy for the thermal degradation using other approaches.

Assuming that the exponential is significantly larger than the unit, the expression that describes the temperature dependence of the thermal residual mass becomes:

$$R(T) = \frac{A}{HD}\exp\left[\left(\frac{E_A^{(S)}}{K_B T}\right)\right] \quad (7')$$

Finally, the temperature derivative of the thermal residual mass is:

$$\frac{dR(T)}{dT} = \frac{A}{HD}\left[\frac{d}{dT}\left(\frac{E_A^{(S)}}{K_B T}\right)\right]\exp\left[\left(\frac{E_A^{(S)}}{K_B T}\right)\right] \quad (7'')$$

Connections to existing theories and models

A simple connection between time evolution and temperature evolution of the mass is recognized by most models on the TGA data. While this does not imply mathematically the dependence suggested here t = t(T), this approach provides the most direct path to transforming the time kinetics into a temperature-related evolution.

Many theoretical approaches to the mathematical modeling of thermograms are consistent with the following differential equation [18], [19], [20]:

$$\frac{\mathrm{dR}}{\mathrm{dT}} = \left[\mathrm{F(R)}\right]\left[\frac{\mathrm{A}}{\mathrm{H}}\exp -\left(\frac{\mathrm{E_A}}{\mathrm{K_B T}}\right)\right] \quad (8)$$

It was assumed that it is possible to separate the time and the temperature contributions of the residual mass (time) function, r(t). The temperature contribution is reflected by the Arrhenius term A exp-(E_A/(RT)) while the time contribution reflects the chemical reaction rate (which may be expressed as $d\gamma/dt=k\gamma^n$, where n is the reaction order) are embedded in the heating rate H and eventually within the function F(R). F(R) is a function of the thermal residual mass that eventually may contain some of the chemical details of the thermal degradation process. Ideally, F(R) does not depend on time but may involve "averaged out" contributions related to the actual chemical reaction paths

By comparing the equation (7") to the existing and accepted mathematical expression (8), the following equivalences are suggested:

$$\mathrm{F(R)} = \frac{1}{D}\left[\frac{d}{dT}\left(\frac{E_A^{(S)}}{K_B T}\right)\right] \quad and \quad E_A^{(S)} = -\left|\delta E_A\right| \qquad (8')$$

It is noticed that by comparing the derived expression with the existing ones, it is concluded that the parameter δ that enters into the definition of the sigmoid activation energy should be negative. The result may be explained by observing that this parameter is related to the time evolution of the residual mass, and longer time implies smaller time (and thermal) residual masses.

The Friedman approximation [15] is obtained by rearranging equation (8):

$$H\frac{dR}{dT} = \left[F(R)\right]\left[A exp - \left(\frac{E_A}{K_B T}\right)\right] \qquad (8'')$$

Taking the natural logarithm of equation 8" is obtained:

$$\ln\left(H\frac{dR}{dT}\right) = \ln\left[AF(R)\right] - \left(\frac{E_A}{K_B T}\right) \qquad (8''')$$

Therefore by representing ln[H(dR/dT)] versus the reciprocal temperature, a straight line with a slope of $E_A/(K_B T)$ is expected [15], [4], [6]. Thus, the activation energy for the thermal degradation is obtained from the heating rate and thermal conversion rates. While the heating rate H in certain cases does not appear explicitly, the fingerprint of Friedman's approximation is the linear dependence of the thermal conversion rate on the reciprocal temperature [21].

An alternative approximation may be derived based on eq. (8):

$$\ln\left(\frac{dR}{dT}\right) = lnF(R) + \ln\left(\frac{A}{H}\right) + \ln\left[\exp\left(-\frac{E_A}{K_{BT}}\right)\right] \qquad (9)$$

Assuming that ln(dr/dT)≈d/dT(lnr) ≈0, changes eq. 9 to:

$$lnF(R) + \ln\left(\frac{A}{H}\right) + \ln\left[exp - \frac{E_A}{K_B T}\right] \approx 0 \qquad (9')$$

Such an approximation suggests that the thermal residual mass does not change rapidly as a function of temperature. Therefore, the general expression for this thermal degradation is given:

$$\left[lnF(R) + \ln\left(\frac{A}{H}\right)\right] - \frac{E_A}{K_B T} = 0 \quad (9'')$$

Or:

$$lnH = lnAF(R) - \frac{E_A}{K_B T} \quad (9''')$$

This model allows for the theoretical simulation and understanding of the TGA thermograms if data at different heating rates, H, are available. An activation energy E_A, associated with the overall degradation process may be calculated in such a case. Eq. (9''') reveals that the dependence of the lnH versus the reciprocal temperature is a straight line with a slope equal to E_A/K_BT, [21], [1], [4], [6] assuming that A and F(R) are constants. A similar expression was derived by Flynn-Wall-Ozawa (FWO) [15]. More detailed calculations suggested that the actual slope within the Flynn-Wall-Ozawa approximation is 1.052 E_A/R [22], [19] or 0.4567 E_A/R [23], [20], [24], [25] and not precisely E_A/R (where R is the ideal gas constant).

While some authors claimed that this model does not consider the details on the thermal degradation, it is essential to note that F(γ) should not depend explicitly on time or temperature.

EXPERIMENTAL METHODS

Polyethylene oxide (PEO) with a molecular mass of 900 KDa was purchased from Sigma

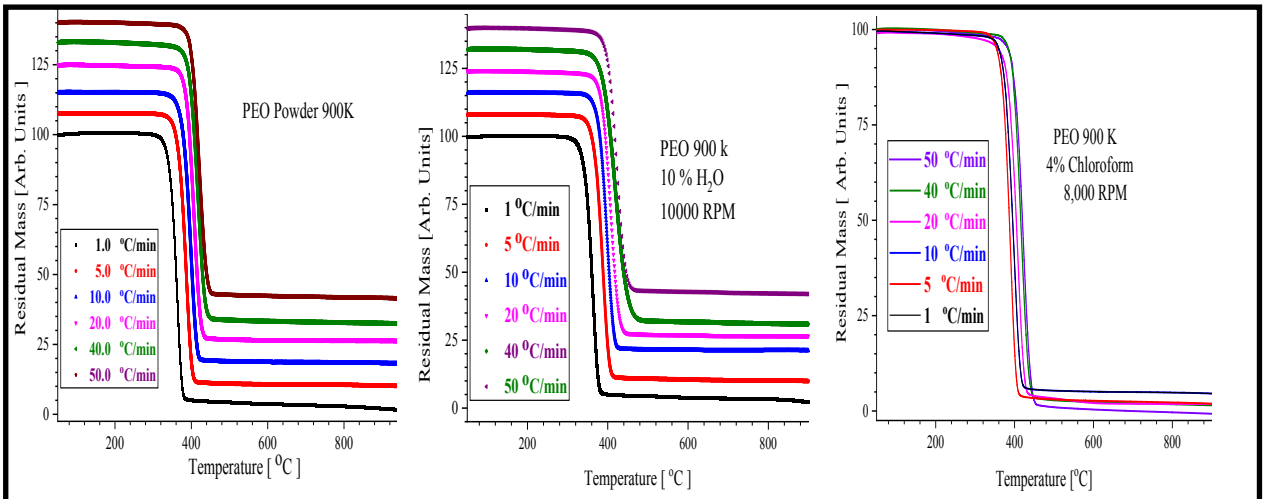

Figure 1. TGA of PEO powder (left), PEO nanofibers from water solution (middle), and PEO nanofibers from chloroform solution (right). Left and middle thermogram were shifted upwards by the same quantity (as the heating rates were increased). Right panel thermograms are represented as recorded (i.e., normalized to 100% and not shifted).

Aldrich. As received, powder PEO was subjected to the TGA analysis in the nitrogen atmosphere at different heating rates. Deionized water solutions of PEO containing 10 % wt. polymer were prepared and homogenized by stirring. Additionally, solutions of 4 % PEO in chloroform were prepared and homogenized using the same procedure as for water solutions. Each of these solutions was centrifugally spun in the air at room temperature using a Fiberio Cyclone L-1000M equipment at a spinning rate of 10,000 rotations/minute (rpm) for the nanofibers obtained from the water solution and a spinning speed of 8,000 rpm for the nanofibers obtained from chloroform solutions. The solvents were removed from nanofibers in a vacuum oven at 50º C for 24 h, to avoid the melting of the polymer and the possible conversion of the mat of nanofibers into a thin film. The PEO melting temperature is reported in the range 55 to 70 ºC [26]. Nanofibers are obtained within a narrow range of rpms and PEO solution's concentration, which depends on the nature of solvent.

The thermal stability of the as purchased PEO powder and PEO nanofibers obtained from water and respectively chloroform solutions by force spinning was studied by thermogravimetric (TGA) experiments using a TG 209 F3 Tarsus Netzsch instrument operating under the nitrogen atmosphere, in the temperature range 50 to 1000 ºC. Measurements with different heating rates from 1 ºC/min to 50 ºC/min were performed on both PEO nanofibers and powder.

RESULTS AND DISCUSSION

Fig. 1 shows the TGA data for PEO powder, with a molecular mass of 900 KDa (left panel), the thermograms for the mats of PEO nanofibers obtained by force spinning of a water solution containing 10 % wt. of the same polymer at a spinning rate of 10,000 rotations per minute (rpms) (middle graph of Fig.1), and the thermograms for the mats of PEO nanofibers obtained by force spinning of a chloroform solution containing 4 % wt. PEO at a spinning rate of 8,000 rpms (see the right graph of Fig.1). The thermal degradations were recorded at various heating rates ranging from 1.0 to 50.0 ºC/min. Thermal degradation experiments were performed in a nitrogen atmosphere. The left and middle graphs of Fig.1 have the thermograms shifted upwards by 8 % for a better view of the effect of the heating rate on the degradation of PEO powder and nanofibers. The right graph of Fig. 1 shows the actual recorded thermograms, after normalization to 100 %, performed by the software of the instrument and no shifting.

As observed from Fig. 1, all thermograms are single simple sigmoids, irrespective of the heating rate and morphology (powder or mats of nanofibers). It is noticed that as the heating rate was increased, the thermograms shifted to higher temperatures. Fig. 2 magnifies Fig.1 for PEO powder and PEO nanofibers obtained from the water solution by focusing on the temperature region, where the strongest mass degradation occurs (temperature ranging from 250 ºC to 500 ºC). The data are shown in Figs.1 and 2 indicate no significant (qualitative) differences between the thermal degradation of PEO powder and PEO nanofibers, irrespective of the nature of the solvent. As observed from Figs. 1 and 2, in all cases, a single sigmoid-like dependence was recorded for the dependence of the (thermal) residual mass on temperature. This dependence is frequently referred to as thermogram.

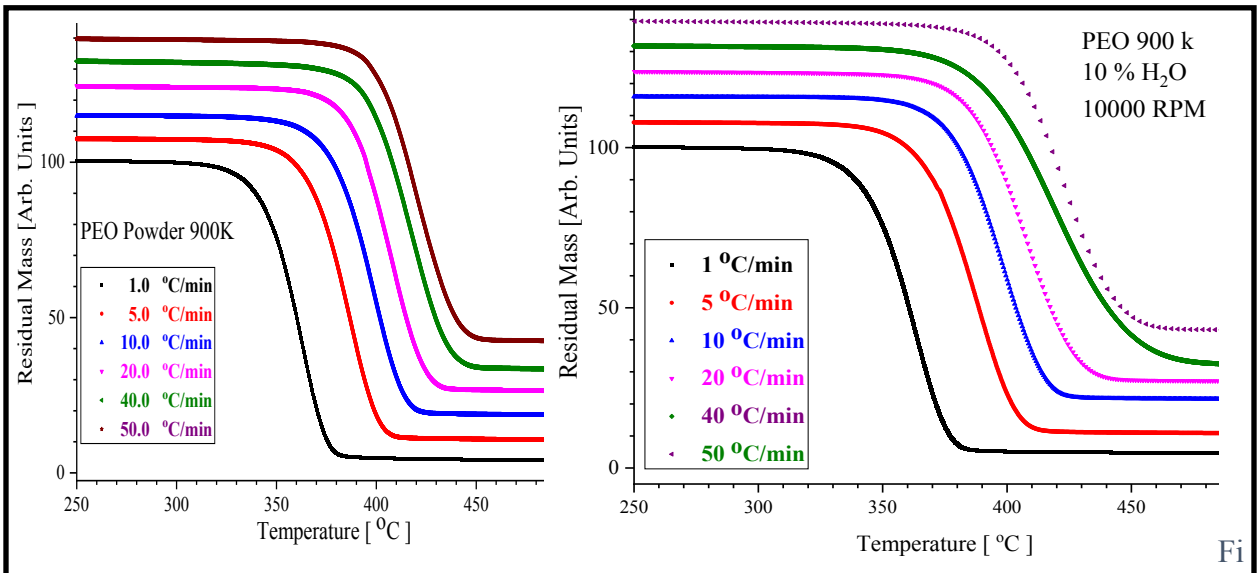

Figure 2. Detail of TGA of PEO powder (left) and PEO nanofibers (right). Each thermogram was shifted upwards by the same quantity (as the heating rates were increased).

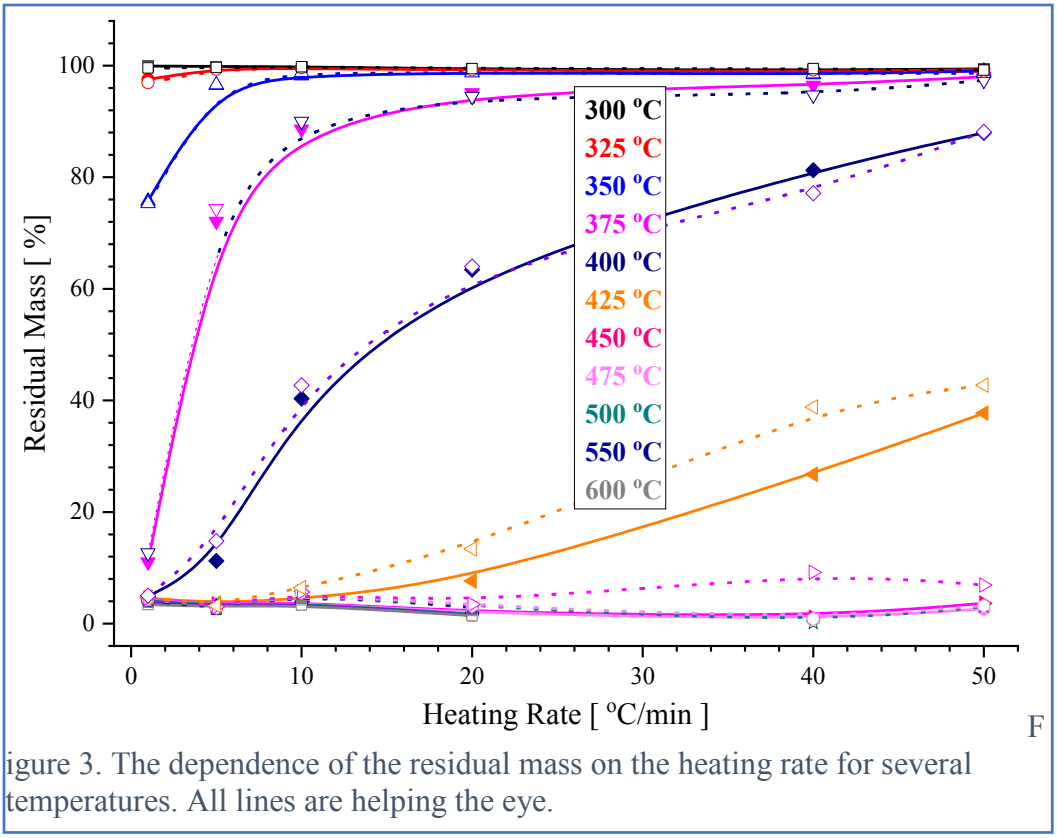

Figure 3. The dependence of the residual mass on the heating rate for several temperatures. All lines are helping the eye.

From Fig. 2, it is noticed that as the heating rate was increased, the inflection temperature shifted to higher values. The dependence of the residual mass dependence on the heating rate at some selected temperatures is shown in Fig. 3 for different heating rates. The data for PEO powder are represented by full symbols and double lines, and the data for PEO nanofibers (from water solutions) are represented by empty symbols and connected by dotted lines. The same color stands for the same temperature; the color and symbol codes are included in Fig. (3). Some differences between powder and nanofibers may be observed in the temperature range where the mass loss is larger.

The simple model suggested in the previous section makes possible the fitting of each individually recorded thermogram by a sigmoid. Consequently, it is assumed that the following equation (which represents a sigmoidal function) may be used to describe the time and temperature evolution of the residual mass:

$$R(T) = \frac{C}{1 + Dexp\left[-\left(\frac{E_A^{(S)}}{K_B T}\right)\right]} \quad (10)$$

Accordingly, eq. (10) defines a quasi-empirical approach that allows for the direct estimation of the "sigmoid activation energy", $E_A^{(S)}$

The actual TGA data were fitted in Origin Pro using the following expression (see eq.11), where R is the thermal residual mass, A_1=C, A_2=D, R=8314 J/(mole•K) with Z representing the baseline correction, E_A measured in J/mole, and S representing the slope correction.

$$f(t) = \frac{A_1}{1 + A_2 \exp\left(-\frac{E_A^{(S)}}{8.3145 * (t + 273.15)}\right)} + Z + S * t \qquad (11)$$

In the previous paragraph, the temperature dependence was introduced via an Arrhenius-like dependence. This allowed for the quick estimation of this overall activation energy. This "sigmoid Activation Energy," $E_A^{(S)}$, may not coincide with other activation energies calculated for the thermal degradation. In contrast with the standard approach [14], [15], this path does not require any knowledge of the thermal degradation process (chemistry), and it does not need data on the thermal degradation processes at different heating rates.

As can be observed in Fig. 4, the proposed equation (eq.11) represents very well the experimental data for both PEO powder and nanofibers. In Fig.4, the experimental data were represented by various symbols for PEO powder (left graph) and PEO mats obtained from water solutions (middle graph), while the best fit was represented by dotted lines. The color identifies

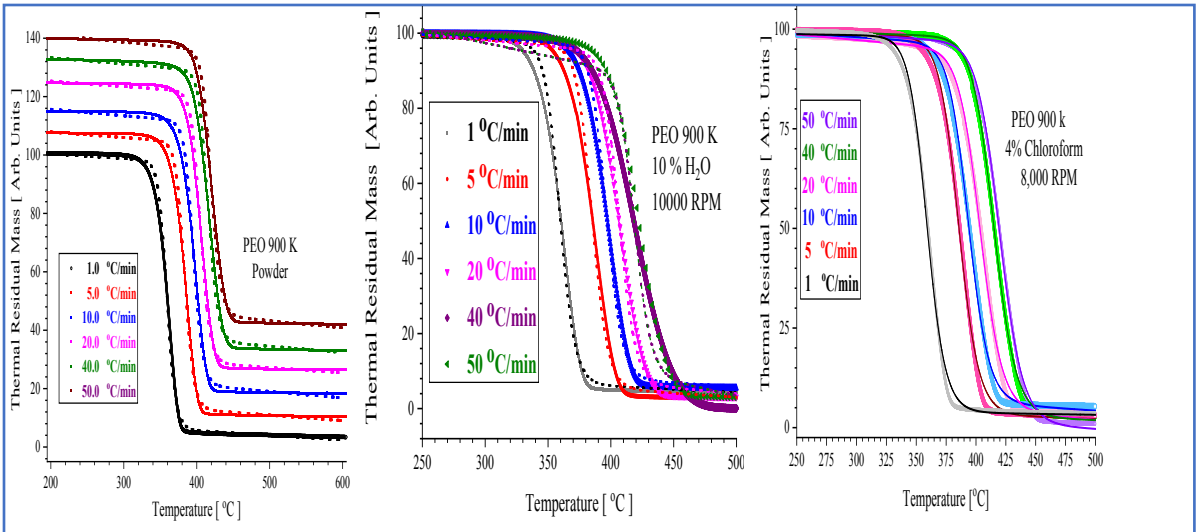

Figure 4. The dependence of the "thermal residual mass" on temperature for PEO powder (left) PEO nanofibers spun from water solution (middle) and PEO nanofibers obtained from chloroform solutions subjected to different heating rates. In the left and middle graphs, the symbols identify experimental data and the dotted lines represent best fits obtained by using equation (11). In the right panel the broader lines represent experimental data, and the narrow darker lines represent the best fits obtained by using equation (11).

the heating rate. The right diagram of Fig. 4 represents the dependence of the residual (thermal) mass on temperature for the mats of nanofibers obtained from the chloroform solution. The experimental data are represented by wider lines, while the narrower and darker lines represent the best fit. An excellent agreement between the modeling and experimental data was observed for all heating rates and both powder and nanofibers samples, with correlation coefficients better than 0.99 for all dependencies.

From Fig. 5, it is suggested that there are no significant differences between $E_A^{(S)}$ for powder and the mats nanofibers obtained from the water solution, at the same heating rate and that $E_A^{(S)}$ depends on the heating rate, increasing towards an asymptotic value as the heating rate is increased. Fig. 5 shows the dependence of the sigmoid activation energy for mats of PEO obtained from chloroform solutions. It is observed that the sigmoid activation energy exhibits a weak decrease as the heating rate is increased. It is noticed that the sigmoid activation energy from PEO mats obtained from water solution is significantly larger than the sigmoid activation energy of PEO mats obtained from chloroform solutions. Such results-although surprising- are not unexpected

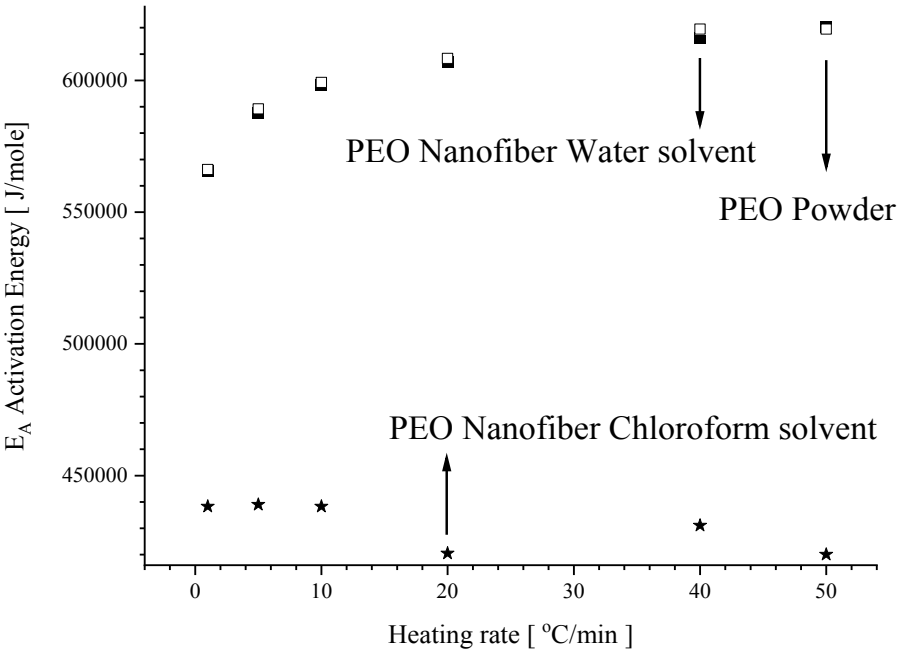

Figure 5. The dependence of the Sigmoid Activation Energy on the heating rate for PEO powder and PEO nanofibers force spun from water solutions and PEO nanofibers force spun from chloroform solutions. All samples derived from the PEO powder with a molecular mass of 900 K.

Many authors reported important information derived from recorded thermograms, such as the temperature at which the thermal residual mass reached a particular value [27], [28]. Frequently, such a temperature was estimated for a thermal residual mass of 50 % [28]. It is the opinion of the authors that such information is empirical and does not carry any physical significance. The sigmoid line shape of thermograms indicates that their first order derivatives with respect to the temperature possess an extremum point, which corresponds to the inflection point of the actual dependence thermal residual mass versus temperature. The physical significance of the inflection temperature is that at this temperature, the degradation rate (thermal mass loss) is maximum. The rate of thermal residual mass loss is maximum at the inflection point. For a symmetric sigmoid ranging between 0% and 100 %, the inflection temperature is reached for a thermal residual mass loss of 50 %. The deviation of the inflection temperature from 50 % of the thermal residual mass is an intrinsic measure of the deviation of the thermograms from the pure symmetric sigmoid curve.

Fig.6 collects the derivative of the thermograms versus the temperature for various heating rates. The negative sign makes positive (maxim) the extremum of the derivative of the thermograms

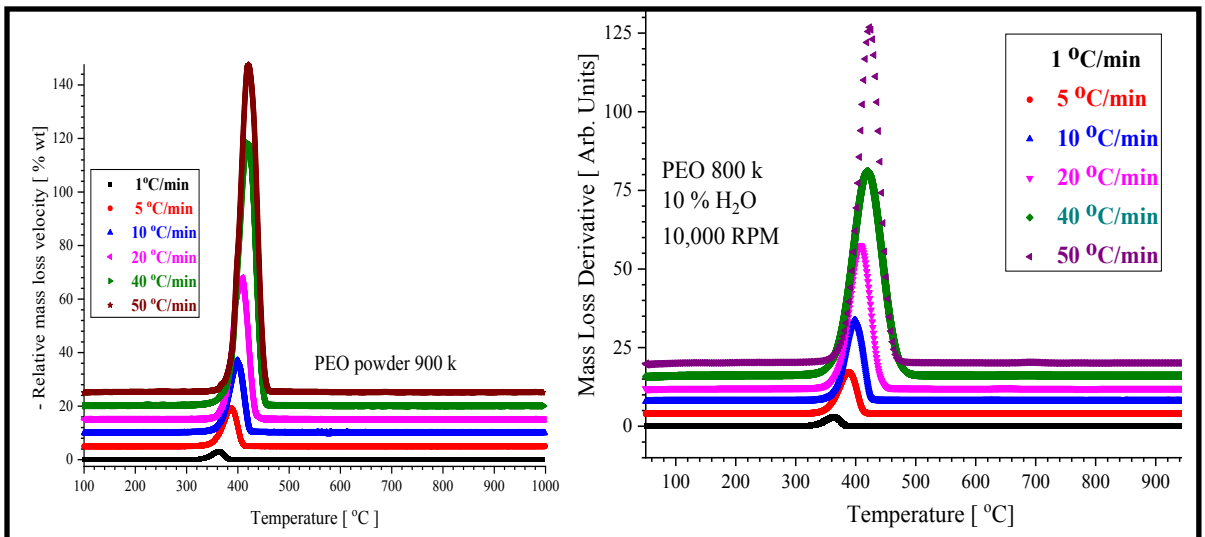

Figure 6. The dependence of the temperature mass loss (conversion) rate on temperature for PEO powder and nanofibers.

versus the temperature. It is noticed that all thermograms show a single extremum (maximum), suggesting a single main degradation process. The position of the maximum defines the temperature at which the mass loss is maximum or the position of the inflection point in the representation of thermal residual mass versus temperature (see Figs. 1 and 2).

The temperature dependence of the "thermal residual mass loss rate" is shown in Figs. 6 and 7 for both powder and nanofibers at various heating rates. All dependencies look similar, showing a single extremum (in this case, a maximum due to multiplication by -1). The single maximum suggests that the thermal degradation of PEO is represented by a single sigmoid-like process, irrespective of the sample's morphology (powder or nanofiber).

A more detailed analysis (see Fig. 7) reveals that as the heating rate is increased, the inflection temperature shifts towards higher values, the Lorentzian shape associated with each thermograms narrows, and that the amplitude of each Lorentzian increases. Quantitative information was obtained by fitting the thermal conversion rates' dependencies on temperatures with Lorentzian-shaped functions. The actual function used to fit the experimental data in Origin Pro is:

$$y=B+S*x+(2*A/PI)*(W/(4*(x-t)*(x-t)+W*W)) \qquad (12)$$

Where y is the residual mass derivative (i.e., residual mass loss rate) at a given temperature t, B is the zero baseline, S describes the slope of the thermogram's derivative, A is the amplitude of

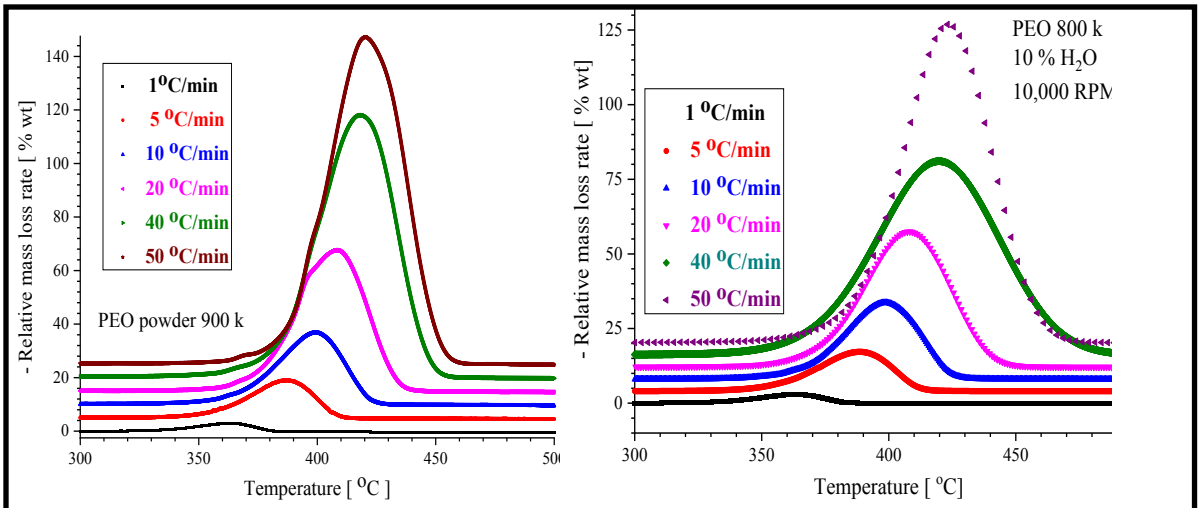

Figure 7. Details of the dependence of mass loss (conversion) rate on temperature for PEO powder and nanofibers.

the derivative, W is the width of the Lorentzian and C is the position of the maximum mass loss rate (velocity) on the OX (or temperature) axis. The fits were excellent and provided the most important parameters, A, W, and C. The integral of the Lorentzian line, S, was also estimated by assuming that the heating rate does not affect the shape.

Now it is easier to notice the effects of the heating rate on the shape of the thermal residual mass loss rate. The increase in the heating rate shifts the position of the temperature, at which the thermal degradation speed is highest, to higher temperatures, narrows the distribution of the relative mass loss velocity versus the temperature, and increases the amplitude of the residual thermal mass loss peak. Eventually, it is noticed that the thermograms are slightly asymmetric; it is speculated that there is a tiny difference between the degradation of PEO in the amorphous and crystalline domains.

A more detailed mathematical analysis was conducted on the derivative of these thermograms. From Figs 6 and 7, it may be concluded that the derivative of the thermograms depends on temperature as a single Lorentzian line shape. Although a weak asymmetry may be noticed, all these derivatives exhibit a single maximum, suggesting that they may be simulated using a single Lorentzian line. This was performed using Origin Pro simulation capabilities in C-Program, corresponding to the equation (12).

The parameters corresponding to the best fit are from Figures 8A and 8B, respectively.

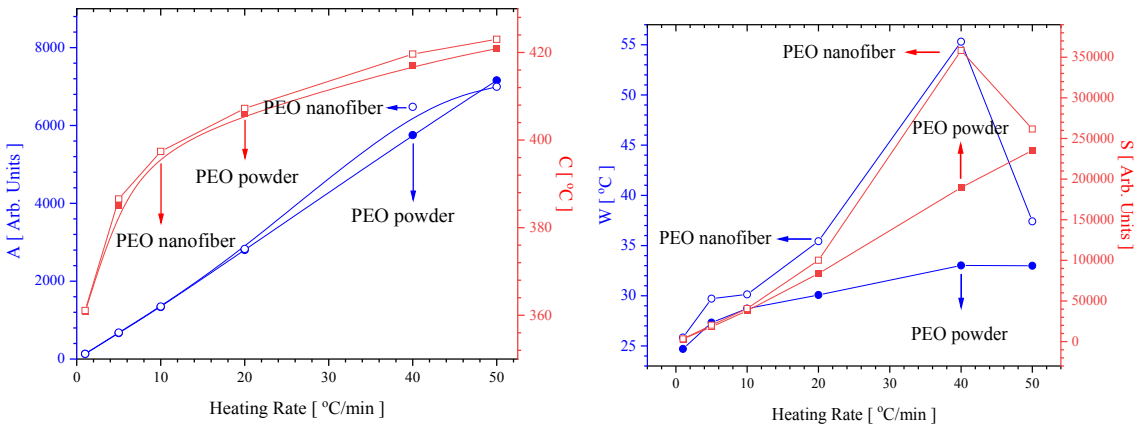

Figure 8. A (Left) . The dependence of A and C on the heating rate. B. right. The dependence of W and S on the heating rate. Empty symbols represent nanofiber, solid symbols represent powder.

It is noticed from Fig. 8A that the amplitude of the mass loss rate, A, depends linearly on the heating rate. Within experimental errors, the area of the mass loss rate also obeys a quasilinear dependence on the heating rate (see Fig. 8B). Fig. 8A shows that the temperature at which the mass loss rate is highest has an asymptotical dependence on the heating rate, with an asymptotic value of about 430 ºC. The widths of these Lorentzians depend asymptotically on the heating rate (increasing as the heating rate increases), with an asymptotic value of about 33 ºC.

Fig.9 shows the dependence of the logarithm of the heating rate versus the reciprocal temperature at different heating rates. These dependencies are characterized by a slope that is proportional to the activation energy of the thermal degradation process within the FWO approximation (see eq. 9). Fig. 10 shows similar data for the PEO nanofibers. In both cases, it is observed that the dependence of lnH versus 1/T is represented with a very good accuracy by straight lines for any conversion ranging between 0.1 and 0.9. The geometrical symbols in Figs.

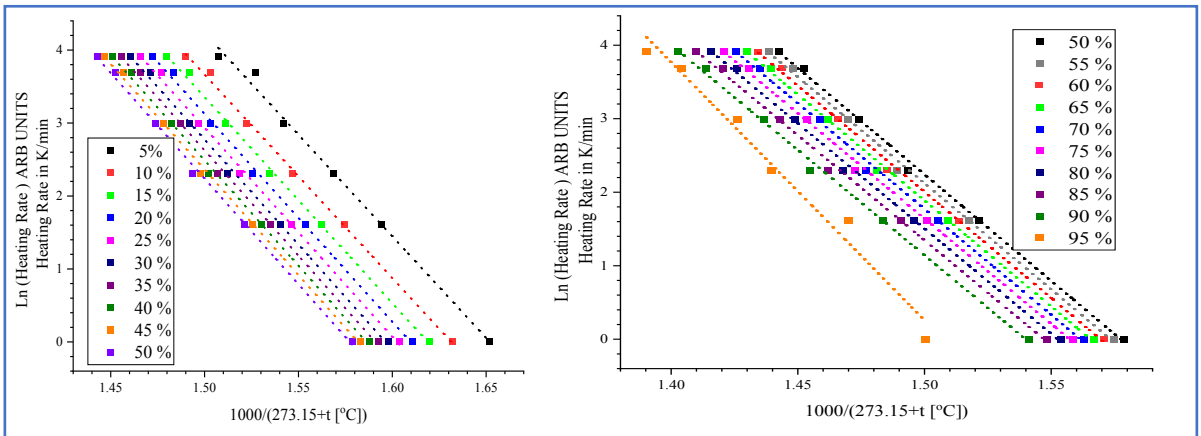

Figure 9 The dependence of the logarithm of the heating rate versus the reciprocal temperature (actually 1000/T) at constant conversion for PEO powder.

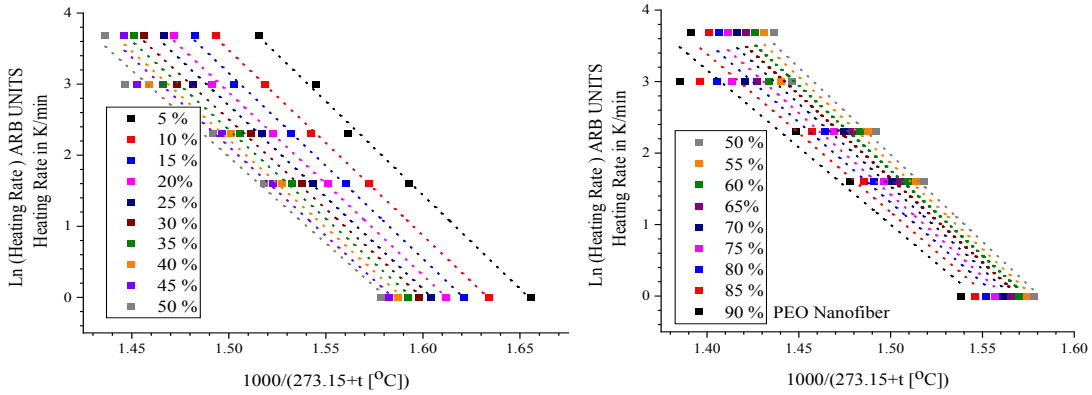

Figure 10 The dependence of the logarithm of the heating rate versus the reciprocal temperature (actually 1000/(273.15+t[°C]) at constant conversion for PEO nanofiber.

9 and 10 are associated with experimental data. At the same time, the dotted lines represent the best fit for the linear dependence of the logarithm of the heating rate versus the reciprocal temperature (at constant conversion). The corresponding activation energies and intercepts were estimated.

Figs. 11 and 12 represent the dependence of the activation energy and intercept on the temperature conversion rate (in normalized values). The inset shows the dependence of the correlation coefficients on the temperature conversion. It is observed that the correlation coefficients are very good for both PEO powder and nanofibers (above 0.95). For PEO powder, the correlation coefficient is better than 0.95 as the temperature conversion ranges between 0.1 and 0.9 and drops very quickly beyond this range. In the case of PEO nanofibers, the correlation coefficient decreases as the temperature conversion increases suggesting additional contributions to the thermal degradation of PEO nanofibers.

The activation energies and the intercepts exhibit similar dependencies on the time conversion for both PEO powder and mats nanofibers (from water solution), although their shapes are different. For PEO powder, the average activation energy is about 240 kJ/Mole, while for PEO nanofibers obtained from aqueous solutions, the average activation energy is about 200 kJ/Mole.

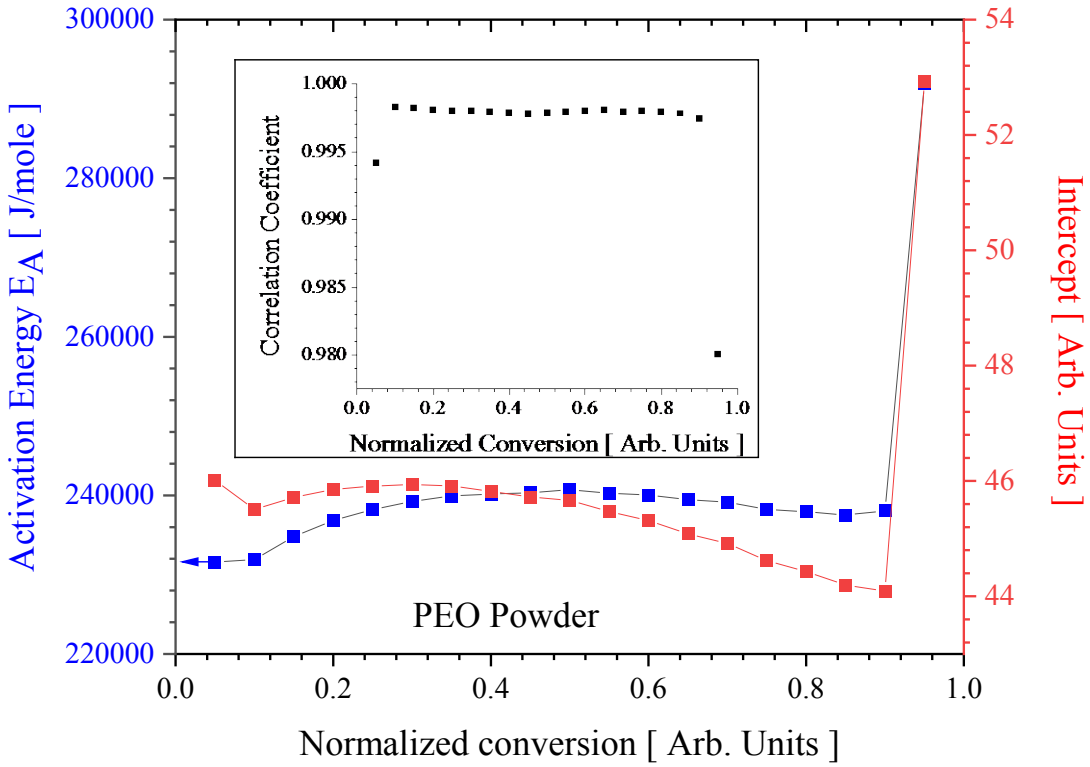

Figure 11. The dependence of the activation energies and the intercepts on the time conversion for PEO powder. The inset shows the dependence of the correlation coefficient on the temperature conversion

CONCLUSIONS

A new semiempirical equation based on a sigmoid-like equation was suggested to analyze TGA data (i.e., for the fitting of the dependence of the residual thermal mass versus temperature). The fitting procedure provides an essential parameter: the sigmoid activation energy.

The sigmoid activation energy may be calculated for each heating rate (i.e., from a single thermogram) and does not depend on the details of the actual chemical, thermal degradation process.

How is this possible? The answer exists in the sigmoidal shape. The general phenomenology of the sigmoid shape is the competition between two processes (for example, a generation process in the short term and a recombination process in the long term). Such dependence may be

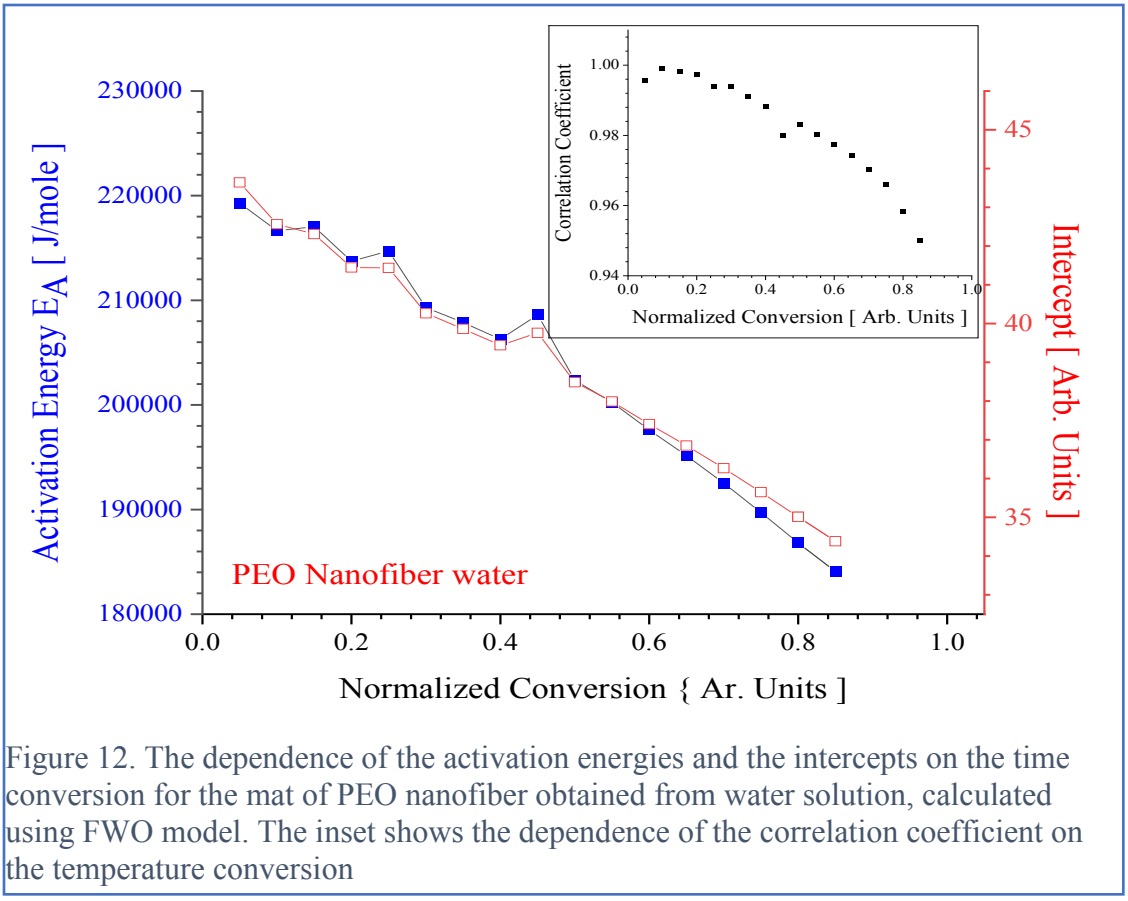

Figure 12. The dependence of the activation energies and the intercepts on the time conversion for the mat of PEO nanofiber obtained from water solution, calculated using FWO model. The inset shows the dependence of the correlation coefficient on the temperature conversion

observed for some chemical processes (some of them involved in thermal degradation). For the simplest process triggered by the thermal degradation, which is the first-order rate process, the sigmoid is not typically considered as it is assumed that the reservoir for this process is infinite. Surprisingly, just by the recognition of the fact that the reservoir is finite, we are forced to acknowledge the need for a sigmoid-like dependence. Hence, the sigmoid covers finite one-dimensional rate processes and processes that involve competition between two opposing factors such as generation and recombination (in some instances, transfer processes may be included). The thermogram is an envelope for all these processes, which frequently degenerates into a single sigmoid-like dependence. Sometimes a superposition of two or more sigmoids may be required to explain and fit the as recorded thermograms. However, it is essential to observe that such a simple dependence is expected for degradation processes occurring in an inert atmosphere.

It was shown that the proposed equation describes the experimental data with excellent accuracy and that the estimated sigmoid activation energies increased as the heating rate was increased for both PEO and mats of nanofibers obtained from water solutions. A different behavior was

noticed in the case of mats of PEO obtained from chloroform solutions. The complex effect of solvents on PEO features [16], including PEO nanofibers was reported earlier [17].

The estimated average sigmoid activation energy for PEO powder and mats of PEO (from water solutions) was approximately 600 kJ/mole. Although these are rather large values, it is important to remind that activation energies for PEO, calculated from TGA data using the kinetic model, were reported to range between 550 kJ/mole (for PEO50 and A0.5) and 591 kJ/mole (for PEG and A0.5) [29].

The FWO method applied to the same experimental data resulted in an average activation energy of about 240 kJ/mole for PEO powder. The activation energy calculated using the Flynn–Wall–Ozawa (FWO) model was reported to increase as the molecular mass of the PEO is increased, ranging from 110 to 210 kJ/mole.

The discrepancy between the sigmoid activation energy and the average activation energy (from FWO) appears significant, but it is important to note that it was never claimed that the sigmoid activation energy is identical to the activation energy. Even more, some authors suggested that the slope of the FWO fit was not precisely the activation energy for the thermal degradation process. If the corrected slope was 0.4567 E_A/R, then the corrected FWO activation energy would be about 525 kJ/mole, quite close to the sigmoidal activation energy. A path to reconcile the discrepancy is to assume that the standard analysis implies the measurement of the smaller activation energy, while the proposed approach is consistent with a slope of 0.4567 $E_A^{(S)} = E_A^{(measured)}$. $E_A^{(measured)}$ is calculated assuming that the slope of the graph of the logarithm of the heating rate (in relative units) versus the reciprocal (absolute) temperature is E_A/R (which is the activation energy). The sigmoid activation energy appears to be consistent with the definition of the slope Ea/R provided by the FW0 model.

The TGA data are sensitive to the nature of the solvent used to obtain the nanofibers of PEO. This was discussed in detail within this manuscript.

In contrast to the sigmoidal activation energy (for PEO powder and PEO mats obtained from water solutions), the activation energy calculated for PEO mats obtained from water solutions, within the Flynn-Ozawa-Wall approach, decreased with increasing temperature conversion. The activation energy for PEO powder (estimated within Flynn-Ozawa-Wall) showed a more complex behavior, with a weak increase as the thermal residual conversion was increased from

0.15 to 0.30, followed by a weak decrease as the thermal residual conversion was increased above 0.3.

The most important advantage of this approach is that it does not require the details of the thermal degradation process and does not need an independent study of the thermal degradation at different temperatures. Further research is needed to understand properly the strength, the limits, and the weaknesses of this approach. A more detailed analysis of the TGA in polystyrene is in work.

ACKNOWLEDGEMENTS

This work was supported by the NSF DMR 2122178 (URGV-UMN PREM)

REFERENCES

[1] G. V Theodosopoulos, C. Zisis, G. Charalambidis, V. Nikolaou, A.G. Coutsolelos, M. Pitsikalis, Synthesis, characterization and thermal properties of poly(ethylene oxide), PEO, polymacromonomers via anionic and ring opening metathesis polymerization, Polymers (Basel). 9 (2017). doi:10.3390/polym9040145.

[2] DK. Chattopadhyay, D.C. Webster, Progress in Polymer Science Thermal stability and flame retardancy of polyurethanes, Prog. Polym. Sci. J. 34 (2009) 1068–1133. doi:10.1016/j.progpolymsci.2009.06.002.

[3] Z. Ahmad, N.A. Al-Awadi, F. Al-Sagheer, Morphology, thermal stability and visco-elastic properties of polystyrene-poly(vinyl chloride) blends, Polym. Degrad. Stab. 92 (2007) 1025–1033. doi:10.1016/j.polymdegradstab.2007.02.016.

[4] F. Bezgin, K. Demirelli, Synthesis, characterization and thermal degradation kinetics of photoresponsive graft copolymers, J. Thermoplast. Compos. Mater. 29 (2016) 1135–1150. doi:10.1177/0892705714563114.

[5] A. Stanciu, V. Bulacovschi, V. Condratov, C. Fadei, A. Stoleriu, S. Balint, Thermal stability and the tensile properties of some segmented poly(ester-siloxane)urethanes, Polym. Degrad. Stab. 64 (1999) 259–265. doi:10.1016/S0141-3910(98)00198-0.

[6] K. Chrissafis, K.M. Paraskevopoulos, S.Y. Stavrev, A. Docoslis, A. Vassiliou, D.N. Bikiaris, Characterization and thermal degradation mechanism of isotactic polypropylene/carbon black nanocomposites, Thermochim. Acta. 465 (2007) 6–17. doi:10.1016/j.tca.2007.08.007.

[7] M. Chipara, K. Lozano, A. Hernandez, M. Chipara, TGA analysis of polypropylene-carbon nanofibers composites, Polym. Degrad. Stab. 93 (2008) 871–876. doi:10.1016/j.polymdegradstab.2008.01.001.

[8] S. Ma, J. Lu, J. Gao, Study of the low temperature pyrolysis of PVC, Energy and Fuels. 16 (2002) 338–342. doi:10.1021/ef0101053.

[9] S. Bocchini, A. Frache, G. Camino, Polyethylene thermal oxidative stabilisation in carbon nanotubes based nanocomposites, Eur. Polym. J. 43 (2007) 3222–3235. doi:10.1016/j.eurpolymj.2007.05.012.

[10] K. Pielichowska, K. Nowicka, Analysis of nanomaterials and nanocomposites by thermoanalytical methods, Thermochim. Acta. 675 (2019) 140–163. doi:10.1016/j.tca.2019.03.014.

[11] N. Ali, D. Chipara, K. Lozano, J. Hinthorne, M. Chipara, Polyethylene oxide—fullerene nanocomposites, Appl. Surf. Sci. 421 (2017) 220–227. doi:10.1016/j.apsusc.2016.11.166.

[12] ARR Adhikari, K. Lozano, M. Chipara, J. Qualls, The effect of carbon nanofiber on the thermo-physical behavior of polyethylene oxide, J. Appl. Polym. Sci. 120 (2011) 3574–3580. doi:10.1002/app.33542.

[13] A. Adhikari, K. Lozano, Effects of carbon nanofibers on the crystallization kinetics of polyethylene oxide, J. Polym. Res. 18 (2011) 875–880. doi:10.1007/s10965-010-9484-3.

[14] AJ de Jesus Silva, M.M. Contreras, C.R. Nascimento, M.F. da Costa, Kinetics of thermal degradation and lifetime study of poly(vinylidene fluoride) (PVDF) subjected to bioethanol fuel accelerated aging, Heliyon. 6 (2020). doi:10.1016/j.heliyon.2020.e04573.

[15] G. Jiang, L. Wei, Analysis of Pyrolysis Kinetic Model for Processing of Thermogravimetric Analysis Data, in: Intech, 2016: p. 13. https://www.intechopen.com/books/advanced-biometric-technologies/liveness-detection-in-biometrics.

[16] T. Sasaki, A. Miyazaki, S. Sugiura, K. Okada, Crystallization of poly(ethylene oxide) from solutions of different solvents, Polym. J. 34 (2002) 794–800. doi:10.1295/polymj.34.794.

[17] Z. Song, S.W. Chiang, X. Chu, H. Du, J. Li, L. Gan, C. Xu, Y. Yao, Y. He, B. Li, F. Kang, Effects of solvent on structures and properties of electrospun poly(ethylene oxide) nanofibers, J. Appl. Polym. Sci. 135 (2018) 1–10. doi:10.1002/app.45787.

[18] A. Dhaundiyal, M.M. Hanon, Calculation of Kinetic Parameters of the Thermal Decomposition of Residual Waste of Coniferous Species: Cedrus Deodara, Acta Technol. Agric. 21 (2018) 75–80. doi:10.2478/ata-2018-0014.

[19] E. Apaydin-Varol, S. Polat, A.E. Putun, Pyrolysis kinetics and thermal decomposition behavior of polycarbonate - a TGA-FTIR study, Therm. Sci. 18 (2014) 833–842. doi:10.2298/TSCI1403833A.

[20] M. Bin Ahmad, Y. Gharayebi, M.S. Salit, M.Z. Hussein, S. Ebrahimiasl, A. Dehzangi, Preparation, characterization and thermal degradation of polyimide (4-APS/BTDA)/SiO 2 composite films, Int. J. Mol. Sci. 13 (2012) 4860–4872. doi:10.3390/ijms13044860.

[21] SC. Oh, W.T. Kwon, S.R. Kim, Dehydrochlorination characteristics of waste PVC wires by thermal decomposition, J. Ind. Eng. Chem. 15 (2009) 438–441. doi:10.1016/j.jiec.2008.11.010.

[22] P.S. Czyk, K. PIELICHOWSKI, I. HAMERTON, J. PIELICHOWSKI, P. STANCZYK, A study of the thermal properties of blends of poly(vinyl chloride) with novel epoxypropanecarbazole-based dyes by tga/ftir, Eur. Polym. J. 34 (1998) 653–657.

[23] S. Shi, X. Zhou, W. Chen, X. Wang, T. Nguyen, M. Chen, Thermal and kinetic behaviors of fallen leaves and waste tires using thermogravimetric analysis, BioResources. 12 (2017) 4707–4721. doi:10.15376/biores.12.3.4707-4721.

[24] N. Huang, Z. Chen, H. Liu, J. Wang, Thermal stability and degradation kinetics of poly(methyl methacrylate)/sepiolite nanocomposites by direct melt compounding, J. Macromol. Sci. Part B Phys. 52 (2013) 521–529. doi:10.1080/00222348.2012.716318.

[25] MK Baloch, MJZ. Khurram, G.F. Durrani, Application of Different Methods for the Thermogravimetric Analysis of Polyethylene Samples Musa, J. Appl. Polym. Sci. 120 (2011) 3511–6518. doi:10.1002/app.

[26] T. Jurkin, I. Pucić, Poly(ethylene oxide) irradiated in the solid state, melt and aqueous solution-a DSC and WAXD study, Radiat. Phys. Chem. 81 (2012) 1303–1308. doi:10.1016/j.radphyschem.2011.12.021.

[27] T. Uma, T. Mahalingam, U. Stimming, Solid polymer electrolytes based on poly(vinylchloride)-lithium sulfate, Mater. Chem. Phys. 90 (2005) 239–244. doi:10.1016/j.matchemphys.2003.11.010.

[28] M. Modesti, A. Lorenzetti, D. Bon, S. Besco, Thermal behaviour of compatibilised polypropylene nanocomposite : Effect of processing conditions, Polym. Degrad. Stab. 91 (2006) 672–680. doi:10.1016/j.polymdegradstab.2005.05.018.

[29] NS. Vrandečić, M. Erceg, M. Jakić, I. Klarić, Kinetic analysis of thermal degradation of poly(ethylene glycol) and poly(ethylene oxide)s of different molecular weight, Thermochim. Acta. 498 (2010) 71–80. doi:10.1016/j.tca.2009.10.005.

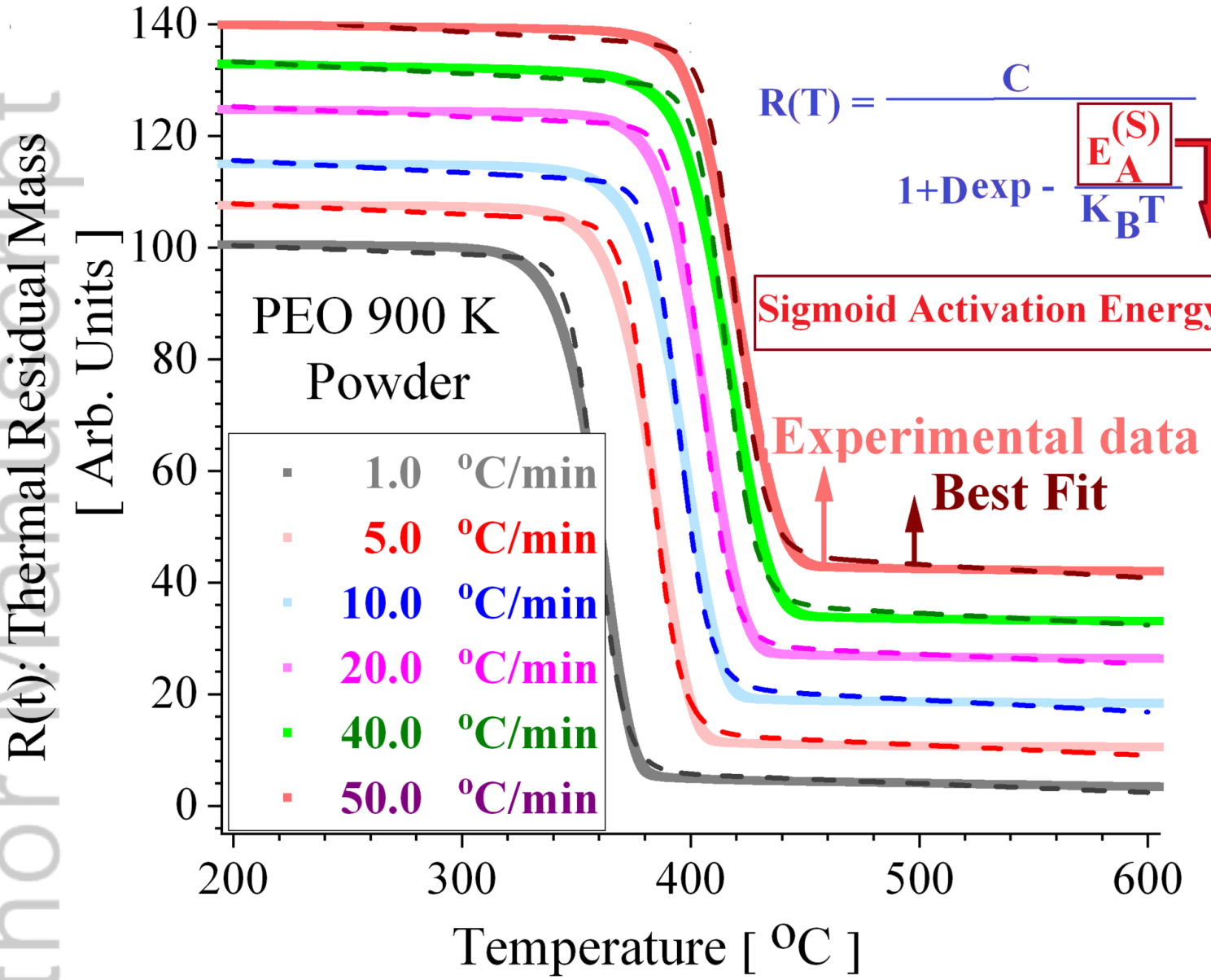

$$R(T) = \frac{C}{1+Dexp - \frac{E_A^{(S)}}{K_B T}}$$

Sigmoid Activation Energy

$$T(K) = t(^{o}C)+273.15$$

$$R(T)=R(t+273.15)$$

APP_52055_graphical abstract_JAPS_FIN1.tif